

## Real-Time Measurement of Thin Film Thickness During Plasma Processing<sup>1</sup>

M. Sarfaty,<sup>2</sup> C. Baum,<sup>2</sup> R. Breun,<sup>2</sup> N. Hershkowitz,<sup>2</sup>  
J. L. Shohet,<sup>2</sup> K. Nagpal,<sup>3</sup> T. L. Vincent,<sup>3</sup>  
P. P. Khargonekar<sup>3</sup>

Received September 26, 1996; accepted May 30, 1997

---

An *in situ* single point two-color laser interferometer is used to monitor in real-time the thickness of thin transparent films during processing. The instantaneous change of film thickness is determined by comparing the measured laser reflection interference to that calculated by a model. The etch or deposition rates of the film are determined within 1–2 seconds. The film thickness is also determined in real-time from the phase difference of the reflected laser intensity between the two laser colors. Use of two-color laser interferometry improves the accuracy of the calculated etch or growth rates of the film considerably. Moreover, the two colors provide a clear distinction between film etching and deposition, which may often occur during the same process, and can not be determined by a single color interferometer. The uniformity of the film's etch or deposition rates across the substrate is monitored by an *in situ* full-wafer image interferometer. The combined use of these two sensors provide instantaneous information of the film thickness, etch or growth rates, as well as time averaged uniformity of the process rates. This diagnostic setup is very useful for process development and monitoring, which is also suitable for manufacturing environment, and can be used for real-time process control.

---

**KEY WORDS:** Laser interferometer; full wafer imaging interferometer; film etching and deposition rates; film thickness; film uniformity; real-time monitoring.

<sup>1</sup>Paper based on the results presented during the workshop of the Engineering Research Center for Plasma-Aided Manufacturing held in Madison, Wisconsin in Spring 1996.

<sup>2</sup>Engineering Research Center for Plasma-Aided Manufacturing, University of Wisconsin-Madison, Madison, Wisconsin 53706.

<sup>3</sup>Department of Electrical Engineering and Computer Science, University of Michigan, Ann Arbor, Michigan 48109.

## 1. INTRODUCTION

Real-time monitoring and control of film etching or deposition is one of the most important goals of thin-film processing. *In situ* sensors, capable of directly monitoring the film's properties in real-time, are the key element to improve the stability of a process to produce the required film quality as well as to increase the product yield. Plasma processing of materials is a relatively complex and sensitive process that depends on a large parameter space. Therefore, real-time monitoring and control are necessary to compensate for changes and drifts that commonly occur in these processes. In order to achieve reliable process control an appropriate *in situ* sensor should be used. The diagnostic sensor has to have the sensitivity, resolution and temporal response to match the desired process objectives. Laser Reflectance Interferometry (LRI), being a noninvasive and nondestructive diagnostic technique, is a very useful and relatively easy to use diagnostic to monitor, in real-time, the thickness of the film.

LRI has long been used to monitor thin film etching<sup>(1-3)</sup> as well as deposition of films such as amorphous silicon<sup>(4)</sup> and diamond<sup>(5)</sup> films, but is commonly used to find the time-averaged etch<sup>(6)</sup> and deposition<sup>(4,5)</sup> rates. In this paper, we extract real-time information from the LRI data, that enables us to calculate instantaneous etching or deposition rates. The real-time algorithm for process rate determination is based on a recent work<sup>(7,8)</sup> that is optimized for transparent thin films to allow fast data processing. The technique is applicable to any type of a thin transparent film composed of single or multi-layer stacks. The instantaneous rate obtained by this sensor, typically within a second, will be used as an input for a real-time process control algorithm. The fast rate calculation is important when a very thin film, fraction of a fringe (single periodic cycle), is grown or etched at a relatively fast rate, which limits the available time for calculation. Also, the dependence of the process rate on various tool parameters, such as rf-power, pressure, flow rates, and gas additives concentrations, enables a quick real-time characterization of the process.

Laser interferometry is commonly used as a single point measurement, thereby, it is insensitive to non-uniformity across the substrate. To monitor the uniformity of the average process rates during film etching or deposition an *in situ* Full Wafer Image Interferometer<sup>(9)</sup> (FWII) is used. The FWII uses a spectrally filtered plasma light emission to detect the interference of light reflected from the top and the bottom of the film. A single wavelength, usually the strong line emission of the plasma, is selected by an interference filter. Optical lenses image the desired area of the film onto a CCD detector capturing the light reflectance from distinct regions on the substrate. The uniformity of the time averaged process rates across the sampled area is

determined from the power spectrum of the recorded periodic data for each of the imaged points. The rates are time averaged over the measured periodic traces, requiring at least one interference fringe.

The two-color LRI and the FWII are used as complementary optical diagnostics. The FWII provides time averaged process rates at many points across the substrate. The multiple-point calculations and statistics are carried out after data acquisition is completed. The two-color LRI sensor determines instantaneous, model-based, process rates, which are calculated continuously with data acquisition while varying the tool parameters. To obtain a similar information with the FWII will require several wafers and longer time to carry multiple step-wise scans of the tool parameters with a couple of periodic fringes at each step. Moreover, in bright plasma discharges the use of external coherent light sources that can be time modulated is advantageous for higher signal-to-noise data.

## 2. EXPERIMENTAL SETUP

The experiments presented here were performed in a cylindrically symmetric Magnetically Confined Inductively Coupled Plasma (MCICP) tool.<sup>(10)</sup> The plasma in the MCICP tool is produced by inductively coupled rf fields (13.56 MHz) generated by a four turn spiral coil antenna. The planar antenna is placed above the 32 cm diameter quartz window that forms the top of the MCICP tool. The upper half of the MCICP side wall is surrounded by a multidipole magnetic bucket of 24 azimuthally alternating magnetic poles (5 kG) equally distributed around the chamber. The magnetic enclosure of the chamber wall enhances the plasma density and improves its uniformity.

A load-lock chamber is connected to the lower half of the chamber. The processed 4-inch wafers are transported to the wafer chuck through a manual gate valve. The wafer chuck is helium backside-cooled and the wafers are clamped to it electrostatically during the plasma processing. The axial motion of the wafer stage transports the wafers from the loading port to the magnetically confined plasma region. Two rf-power supplies and matching networks are used in the system, one is connected to the inductive coil antenna (up to 1.5 kW) and the other to the wafer chuck (up to 0.5 kW). The details of the MCICP system are described in Ref. 8. The computer controlled tool parameters during plasma processing are RF-power to the coil and the chuck, the gas flow rate and pressure.

A two-color, red (632.8 nm, 1.0 mW) and green (543.5 nm, 0.3 mW), He-Ne laser interferometer, shown in Fig. 1, is the *in situ* diagnostic tool used to measure the thin-film thickness in real-time. The periodic modulation of the reflected laser intensity results from interference between light reflected from the top of the film and the interface between the film and the substrate

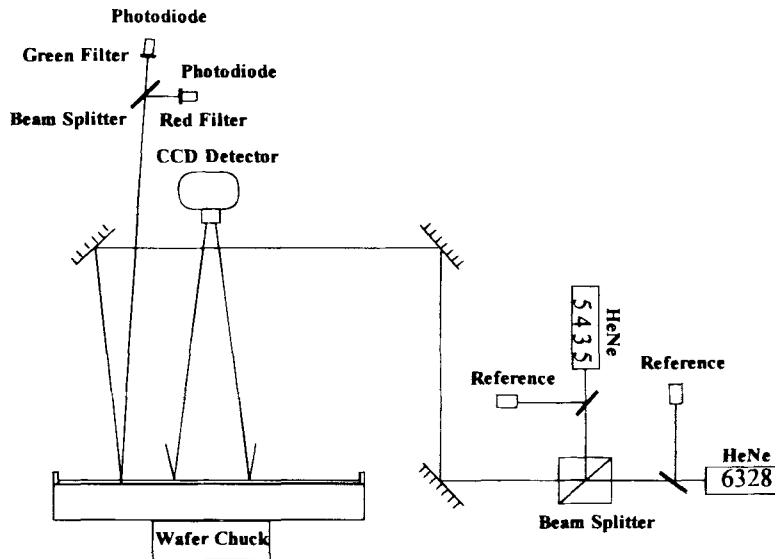


Fig. 1. Schematic of the two-color laser interferometer and the full wafer imaging interferometer (FWII) diagnostic systems.

as the film's thickness is changing. The laser light is bright enough to dominate other sources of stray light from the plasma emission, yet, of a sufficient low energy density not to disrupt the film properties and the involved film chemistry.

A cubic beam splitter is used to merge the two He-Ne laser beams, the red and the green, into a single spot on the wafer. The combined laser beam is introduced and reflected from the wafer surface at  $0.5^\circ$  off normal through the quartz plate on top of the MCICP tool. The reflected laser beam is split into two arms each directed to a photodiode detector. Green and red interference filters select the appropriate wavelength for each of the photodiodes. The red and green interference signals between the top and the bottom of the film on the wafer are digitally sampled at 10 Hz and recorded by a computer using LabView software. The perpendicular orientation of the interferometer beam relative to the processed substrate eliminates the need for diagnostic chamber windows, thus greatly simplifying the installation of such a sensor in an industrial tool equipped with optical access. Also, by keeping the orientation perpendicular to the wafer surface the sensitivity of the sensor to changes in film thickness is maximized. Furthermore, data analysis is simplified as the measured LRI trace is independent of laser polarization and angle of incidence. The incident intensity of both lasers is monitored for signal reference, in practice, however, the intensity was very stable. The nonfocused beam of the combined lasers illuminates a spot size of 1–2 mm

on the substrate. The large transparent quartz window and the assembly of the mirrors provide optical access to any segment of the 100 mm diameter wafer.

As will be shown in the next section, the use of two lasers of different colors, as opposed to one, improves the accuracy of the calculated rate of change of film thickness, and provides a real-time measure of the thin-film thickness as well as distinguishing between film etching and deposition. An *ex situ* multiwavelength ellipsometer is used to determine index of refraction of unknown films and the its constancy after plasma treatment. The film thickness estimated in real-time by the two-color laser interferometer was verified by the *ex situ* ellipsometer at various stages of film etching or deposition.

The uniformity of the process is monitored in real-time across the substrate using a Full Wafer Imaging Interferometer (FWII) 1000-IS manufactured by Low Entropy Systems.<sup>(9)</sup> The FWII consists of a computer controlled CCD detector equipped with an interference filter and imaging optics. The CCD camera and the light collection optics are mounted on top of the MCICP tool, as shown in Fig. 1, collecting reflected light perpendicular to the processed substrate. A 5 nm bandwidth interference filter, usually centered at the strongest line emission of the plasma, is the light source used both to monitor the thin film interference pattern and to detect optical emission etch-endpoint. Each of the 4000 pixels of the CCD detector images a small region on the substrate determined by the imaging optics. The measured periodic modulation of the reflected light intensity is fast Fourier transformed to yield the process power spectrum, i.e., the time averaged etch or growth rates. The information gathered and analyzed from all of the CCD pixels shows the uniformity of the process rates across the sampled area.

### 3. RESULTS AND DISCUSSION

#### 3.1. Laser Reflectance Interference Model

To interpret in real-time the reflected laser interference signal as film thickness changes, a LabView computer program was developed. The computer simulation that models the laser reflectance signal from a generic multilayer film follows the matrix method developed in Ref. 11. A similar approach was made in Ref. 12 for numerical simulation of optical etch rate monitoring. The matrix method reduces any stack of film layers to three layers including the substrate. However, the experiments described in this paper are made with a single film layer deposited on a silicon wafer as shown in Fig. 2. Therefore, the ratio of the reflected to the incident light amplitude is given simply by

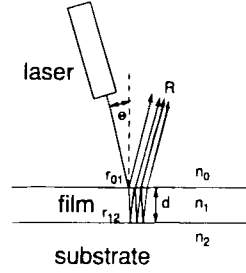


Fig. 2. Thin-film laser reflectance model of a single film.

$$R(\lambda) = \frac{r_{01} + r_{12}e^{-2i\delta_1}}{1 + r_{01}r_{12}e^{-2i\delta_1}} \quad (1)$$

where  $r_{01}(\lambda)$  and  $r_{12}(\lambda)$  are the complex Fresnel reflection coefficients determined by the film and substrate complex indices of refraction,  $n_1$  and  $n_2$ , respectively, at the appropriate laser wavelength.

$$r_{01}(\lambda) = \frac{1 - n_1(\lambda)}{1 + n_1(\lambda)} \quad (2)$$

$$r_{12}(\lambda) = \frac{n_1(\lambda) - n_2(\lambda)}{n_1(\lambda) + n_2(\lambda)} \quad (3)$$

The index of refraction of an unknown film that is deposited on a bare silicon substrate is first determined *ex situ* by a multiwavelength ellipsometer and then entered into the real-time algorithm. The proper index of refraction for each of the laser colors was used in the code. The constancy of the film's index of refraction during plasma deposition or etching was verified by comparing the real-time estimated film thickness with *ex situ* ellipsometry of the films at several different stages of the process. The wavelength and time dependent phase shift between the laser light reflected from the top and bottom of the film,  $\delta_1(\lambda, t)$ , is given by

$$\delta_1(\lambda, t) = \frac{2\pi}{\lambda} n_1(\lambda)d(t) \quad (4)$$

for laser wavelength  $\lambda$ , film index of refraction  $n_1(\lambda)$ , and time varying thickness  $d(t)$ . The phase shift term, as defined in Eq. (4), reflects the time dependent change of the film thickness during processing. The detected laser reflectance intensity  $I_R$  is equal to

$$I_R(\lambda, t) = |R_1|^2 = \frac{r_{01}^2 + 2r_{01}r_{12} \cos 2\delta_1 + r_{12}^2}{1 + 2r_{01}r_{12} \cos 2\delta_1 + r_{01}^2 r_{12}^2} \quad (5)$$

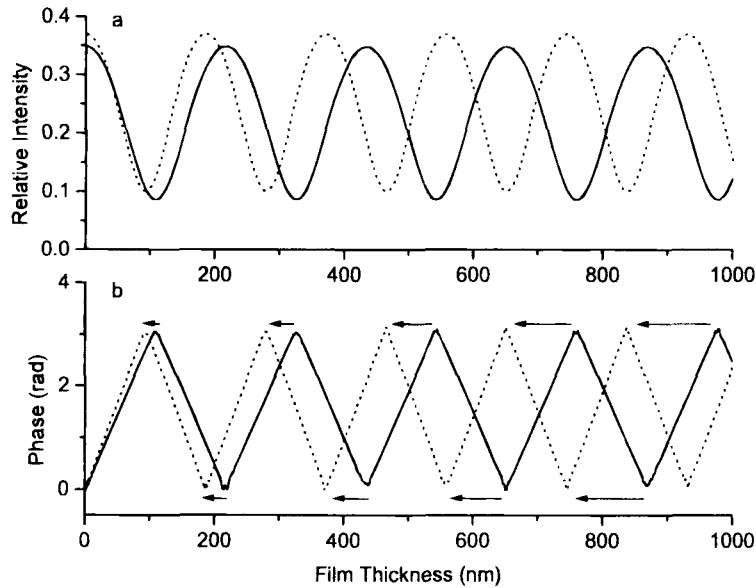
The modeled LRI traces of both the green and the red lasers are shown in

Fig. 3a, for etching/depositing one micron of SiO<sub>2</sub> film on a silicon wafer. The time dependent phase shift,  $\delta_1(t)$ , that accounts for the measured LRI signals is calculated using Eq. (6).

$$2\delta_1(\lambda, t) = \cos^{-1} \left[ \frac{I_R(\lambda, t)(1 + r_{01}^2 r_{12}^2) - (r_{01}^2 + r_{12}^2)}{2r_{01} r_{12} (1 - I_R(\lambda, t))} \right] \quad (6)$$

The time derivative of  $\delta_1(\lambda, t)$ , as long as the index of refraction is time independent [see Eq. (4)] is directly related to the variations of the film thickness during the process. The phase of the LRI traces determined by Eq. (6) for both laser colors as a function of film's thickness is shown in Fig. 3b.

More than having two independent measurements of the film thickness with two colors, the periodicity difference of the two lasers, which scales as  $\lambda/2 n_1(\lambda)$ , improves considerably the real-time estimation of the time dependent film thickness. This is achieved by partially avoiding the relatively flat peak sections of the interference pattern, as shown in Fig. 3a. The flat LRI peaks are less sensitive to film thickness variations, as the observed intensity hardly changes with film thickness. Since the flat peaks appear at different film thickness for each of the laser colors, a selective use of the measured



**Fig. 3.** Calculated laser reflectance traces of red (solid-line) and green (dotted-line) laser interference produced by deposition or etching of 1  $\mu\text{m}$  SiO<sub>2</sub> film on a silicon substrate. (a) The relative intensities of the two laser colors as a function of film thickness; (b) The phase of the two-color laser reflectance traces. The phase difference between the red and the green traces, shown in arrows, at any given phase is a measure of the film thickness.

LRI traces, minimize the contribution of the peaks to the real-time estimate of film thickness variations. Moreover, the phase difference between the LRI pattern of the two laser colors, as seen in Fig. 3b, is directly related to the absolute film thickness. The arrows in Fig. 3b show an example of phase difference between the peaks of the two-color LRI phase trace as a function of absolute film thickness. This information, together with the estimated film etch or deposition rate, provides a real-time measure of the film thickness. The periodicity of the phase difference between the two laser colors for SiO<sub>2</sub> film limits the maximum film thickness that is uniquely determined to ~1.1 microns. Knowing the absolute thickness of the film in real-time eliminates the need for end point detection of film etching, since film thickness can be predicted at any time during the process. Also, the change of the relative phase between the two-color LRI traces makes it possible to distinguish between film etching and deposition, which is not possible when a single-color LRI is used.

For a film of constant index of refraction the LRI technique interprets the measured intensity variations as film thickness changes. The typical noise in the measured LRI signals of ~5% limits the average uncertainty of film thickness to be of the order of 1/10 of a fringe or ~0.5 rad in phase. As mentioned earlier the uncertainty is larger at the flat peaks of the LRI signals and smaller at the linear parts. The corresponding film thickness resolution is  $\lambda/20 n_1(\lambda)$ , which is about 20 nm and 8 nm for SiO<sub>2</sub> and polysilicon films, respectively, monitored by these laser colors. The film thickness resolution is improved for films with index of refraction higher than that of SiO<sub>2</sub> (1.46), as long as the film remains transparent. Also, a shorter laser wavelength improves the thickness resolution by the combined effects of reduced wavelength and increased index of refraction at shorter wavelength.

Using this model, we compare, in real-time, the measured data with the model prediction to determine the film thickness and the instantaneous etch or deposition rate. The peak amplitude of the measured periodic signal may vary during the process and between processes due to changes of window transparency as well as light scattering of the processed substrate. The algorithm therefore follows the peaks of the measured signals and updates their values in real-time to allow accurate process rate calculations. An exponentially weighted moving average filter is used to smooth the measured data. The smooth data is peak scaled to match the peak-normalized LRI model values. A second filter, a single-step-prediction Kalman filter, is used for process rate calculation to prevent large fluctuations in the estimated process rate due to signal's noise. The time derivative of the phase transformed LRI trace provides the process rates. The gain of each of the filters is optimized by the program for each of the laser colors according to their noise level to yield better rate estimates. Modeling and comparison with the measured LRI



signals is carried out simultaneously for the two laser colors. The weighted results of each of the colors are combined to give the instantaneous process rates and film thickness. A more detailed description of the real-time rate computation algorithm will be given in future publication.

### 3.2. Real-Time Measurements of Film Etching and Deposition Rates

The two-color laser interferometer is used to determine, in real time, the etch rate of  $\text{SiO}_2$  film at several antenna and chuck power levels. The red and green laser reflectance traces are shown in the upper part of Fig. 4. During the first 220 seconds the 0.96 micron  $\text{SiO}_2$  film is etched by the  $\text{CHF}_3$  plasma. In this run the gas pressure and flow rate are fixed at 3 mTorr and 33 sccm, respectively. The wafer chuck is rf self-biased using 75 W of input power, while the antenna power is varied between 0.5 kW, 0.75 kW and 1.0 kW. The periodicity difference between the red and the green LRI traces as well as their time dependent changes with rf antenna power are clearly seen from the raw interference data. From  $t = 220$  seconds (see Fig. 4) the laser reflectance remained flat for the next 50 seconds, indicating a complete etch

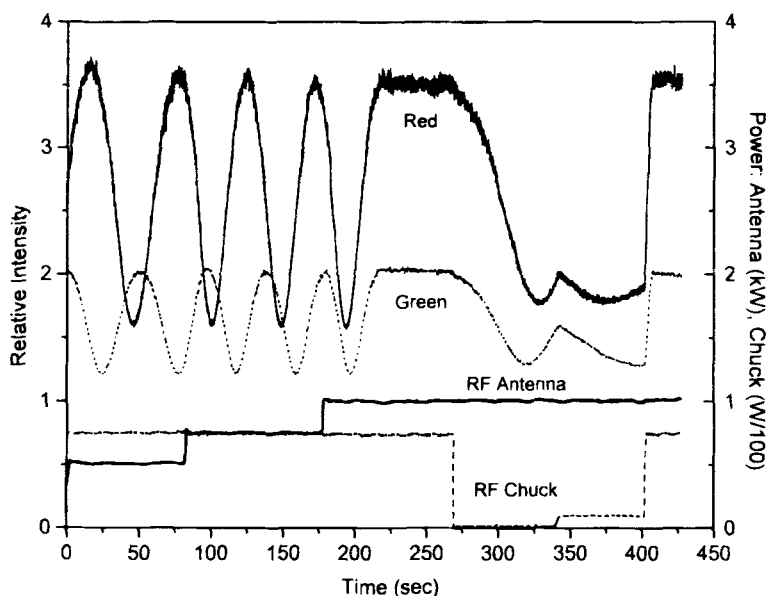


**Fig. 4.** Red (solid-line) and green (dotted-line) laser reflectance measured during plasma etching of a 0.96  $\mu\text{m}$   $\text{SiO}_2$  film. The  $\text{CHF}_3$  processing gas is kept at a pressure of 3 mTorr and flow rate of 33 sccm. The chuck (dashed-line) and antenna (solid-line) RF-power at various process stages. Chuck rf power is set at 75 W while the antenna power is varied from 0.5 to 1.0 kW. A  $\text{CF}_x$  film is deposited on the silicon wafer when the chuck power is turned off. This film is etched when the chuck power is higher than 5 W.

of the  $\text{SiO}_2$  film. At  $t = 270$  seconds, the chuck power is turned off while the rf antenna is kept at 1.0 kW. When the chuck power is turned off, a  $\text{CF}_x$  film starts to grow on the bare silicon wafer. This film is etched slowly when 10 W of RF-power is applied to the wafer chuck and much more rapidly at 75 W.

The instantaneous etch rates of  $\text{SiO}_2$ , calculated for the first 220 seconds data of the process described in Fig. 4, are shown in Fig. 5. The RF-power applied to the wafer chuck is 75 W and the corresponding rf antenna power is plotted below the etch rates. The dashed and dotted lines represent the calculated instantaneous etch rate using the green and the red lasers, respectively. The red laser trace, shown in Fig. 4, is noisier than the green laser which accounts for the difference seen in the estimated etch rate. The etch rate, shown in thick solid line, is the weighted combination of the separate etch rate results of the two lasers. Etch rate variations of 5–10% observed during constant rf antenna power stage are typical to data with  $\sim 5\%$  noise. Also, the initial slow rise time of the red laser etch estimation is due to the flat peak of the original red LRI trace, see Fig. 4, which is less sensitive to etch rate changes and is usually more noisy. The uncertainty in the final (thick line) etch rate calculation is half that of the red laser for this particular run. The time response of the etch rate calculation is 5–10 seconds as seen

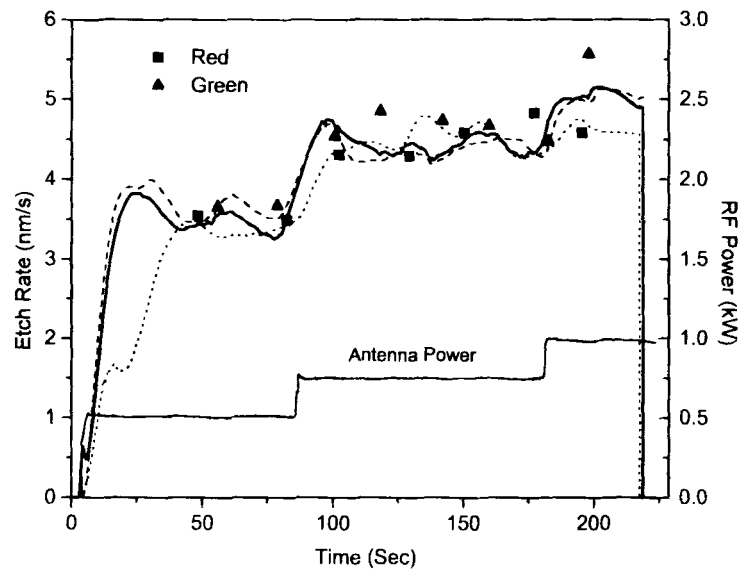


**Fig. 5.** Real-time etch rates of  $\text{SiO}_2$  film as a function of antenna rf power at a constant chuck power of 75 W. The time dependent etch rates calculated with a single green (dashed-line) and red (dotted-line) laser reflectance and the combined rate (solid-line) are compared. The time averaged etch rates every half fringe for both colors are shown as solid points.

near the new set points of the antenna power. A faster response can be obtained but it introduces larger variations of the estimated etch rate for the current quality of data points. The time response can be optimized to various process rates by improving signal-to-noise ratio and varying the data sampling rate. The dark data points shown in Fig. 5 are the time averaged etch rates determined every half fringe of film etching for both laser colors. The rate variations between the two colors and from the instantaneous values are mainly due to peak detection uncertainties.

The instantaneous thickness of the etched  $\text{SiO}_2$  film, calculated in real-time, is given in Fig. 6 for the same first 220 seconds of data of the process described in Fig. 4. The film thickness is derived from the phase difference between the LRI traces of the red and green lasers and the instantaneous etch rates given in Fig. 5. The changes in rf-power to the antenna are shown as vertical lines.

The two-color laser interferometer can be used, in real-time, to evaluate process rates as a function of any desired tool variable. In Fig. 7 the real-time etch rate of  $\text{SiO}_2$  is determined for a time varying wafer-chuck power. The red and green LRI data are the periodically varying traces shown in Fig. 7 while the chuck power is the linear ramp rising from 0 W to 120 W. During the first 60 seconds, the small initial fringe in Fig. 7 corresponds to a  $\text{CF}_x$  film that is deposited on top of the original  $\text{SiO}_2$  film at chuck power below

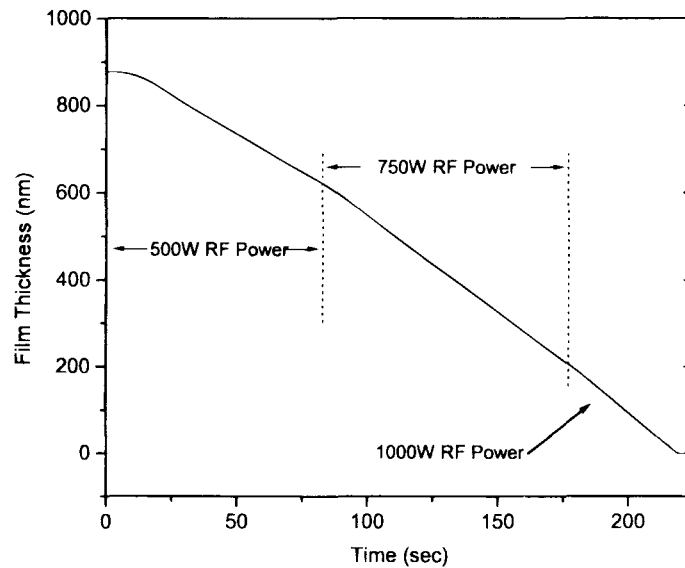


**Fig. 6.** Real-time thickness of the etched  $\text{SiO}_2$  film determined by the instantaneous etch rates and the phase difference between the traces of the two-color laser reflectance. The time points of antenna rf-power changes are shown as vertical lines.

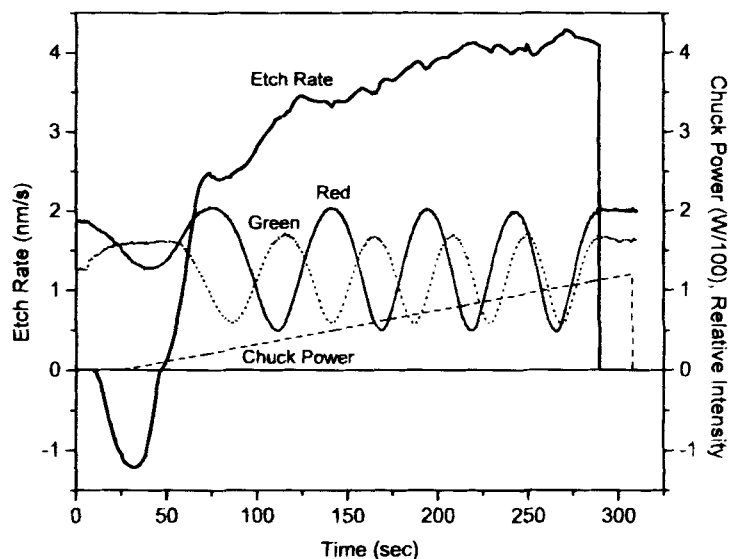


**Fig. 7.** Real-time calculated etch rates of SiO<sub>2</sub> film (thick solid-line) for a linearly rising chuck power from 0–120 W and a fixed antenna power of 750 W. The CHF<sub>3</sub> processing gas is set at a pressure of 4 m Torr and flow rate of 30 sccm. Also shown are the red (solid-line) and green (dotted-line) laser interference measured during the process characterization run.

5 W and is etched at higher chuck power. Film deposition is represented by negative etch rate and etching by positive values. At  $t = 60$  seconds the reflected intensity reaches the initial value, which is the beginning of the etching of the SiO<sub>2</sub> film. The dependence of SiO<sub>2</sub> etch rate on chuck power is determined, in real-time, in one continuous run using a single wafer. Similarly the rf power to the antenna, the gas flow rate and pressure, gas additives, etc. were varied during the process, and the etch or growth rate of the associated film was calculated in real-time. This procedure simplifies and considerably reduces the time required to develop, characterize, and optimize a process.

A typical process of CF<sub>x</sub> film deposition is shown in Fig. 8 for fixed tool conditions. The antenna power is set at 1.0 kW and no rf power is applied to the wafer chuck. The CHF<sub>3</sub> gas flow is fixed at 40 sccm and the pressure at 4 m Torr. The instantaneous deposition rate of the CF<sub>x</sub> film varies in the range of 1.8–2.0 nm/s and is etched at a rate of ~16 nm/s when a constant 75 W of RF-power is applied to the wafer chuck. The values for the refractive index and extinction coefficient of the CF<sub>x</sub> film at a wavelength of 633 nm are 1.402 and 0.00447, respectively. These values were measured by an *ex situ* multi-wavelength ellipsometer.

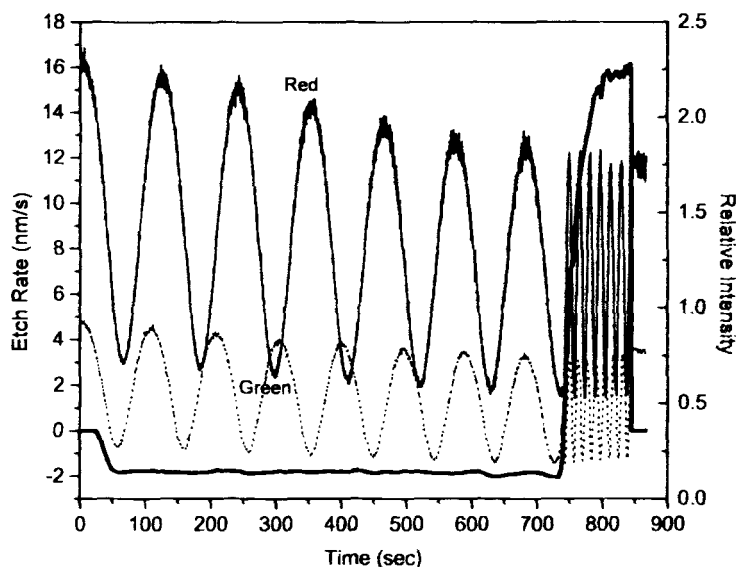


**Fig. 8.** Real-time process rates (thick solid-line) calculated during deposition and etching of  $\text{CF}_x$  film using  $\text{CHF}_3$  at a pressure of 4 mTorr and flow rate of 40 sccm. The antenna power is constant at 750 W; the chuck power is set to zero during film deposition ( $t < 735$  sec.), and 75 W during film etching ( $t > 735$  sec.). The red (solid-line) and green (dotted-line) laser reflectance traces measured during the process are shown.

The reflectance of both of the lasers decrease during the relatively long (720 seconds) deposition time, and maintained at the same peak intensity during the relatively fast etching phase (100 seconds). The decrease of the light intensity with time may result from film absorption, however, the reflected intensity does not reach the initial value after the film is completely etched. Moreover, film absorption will manifest in LRI traces as a shrinking envelope similar to wave damping traces of oscillating waveforms. Also, the measured low extinction coefficient of the  $\text{CF}_x$  film can not explain the observed decrease of the LRI traces. Therefore, it is more likely that laser scattering due to roughening of the film's surface<sup>(13)</sup> or of the quartz window, as well as coating of the window during the relatively long time scales, is the reason for the observed drop in the LRI intensity during film deposition. A comparison similar to the study made in Ref. 13, between surface roughness measured by atomic force microscopy and LRI traces, is required to determine the reason for this behavior. However, the instantaneous deposition rates can still be derived from these traces by re-scaling the measured LRI envelope to the peak-normalized model traces. The computer program detects and updates in real-time, the peaks of the measured LRI traces and re-scales them prior to the comparison with the model traces. The re-scaling of the measured

LRI is very important to avoid errors in the calculated etch or growth rates of the film. Without proper peak scaling the phase information of the measured LRI traces is misinterpreted and the comparison to the normalized model will be incorrect.

The deposition rate uniformity of the  $\text{CF}_x$  film measured by the FWII across 100 mm of wafer diameter is shown in Fig. 9. The CCD detector of the FWII is placed above the MCICP tool, see Fig. 1, having a perpendicular view of the wafer surface. The results are analyzed after 18 minutes of film deposition by performing a fast Fourier transform of the measured light reflectance from each of the 425 selected regions of the wafer. In this run the average growth rate of the film over  $\sim 10$  fringes is  $403 \text{ \AA}/\text{min}$  ( $0.67 \text{ nm}/$

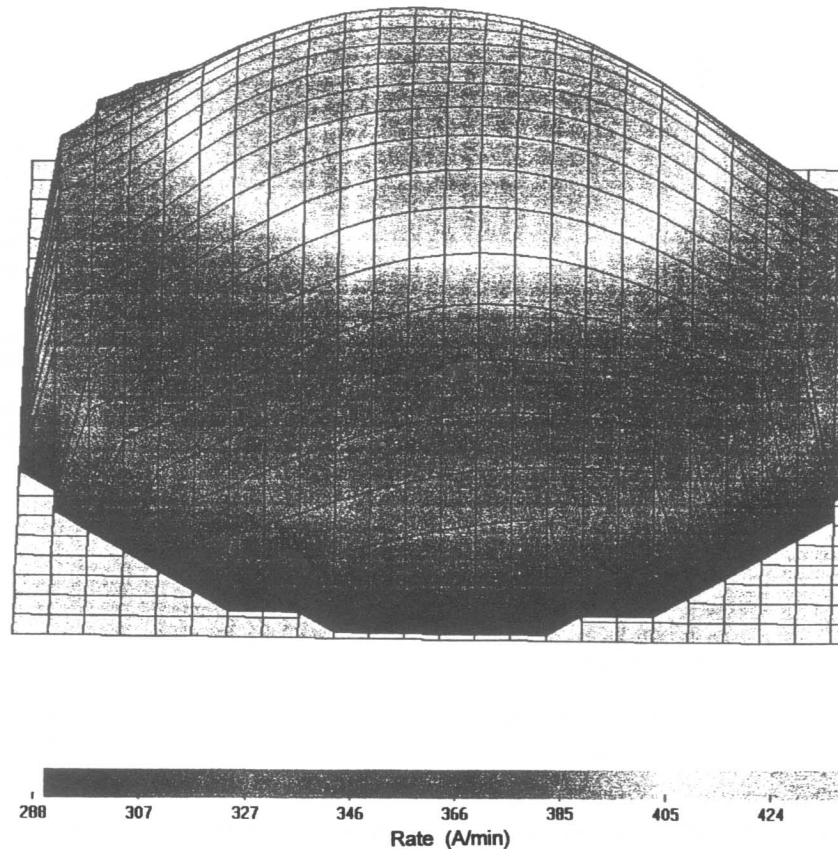


**Fig. 9.** The uniformity of the  $\text{CF}_x$  film deposition measured *in situ* by the FWII. The average deposition rate is  $403 \text{ \AA}/\text{min}$  with a standard deviation of  $28 \text{ \AA}/\text{min}$  or 7% over the 100 mm wafer diameter.

s) with a standard deviation of 7%. Similar instantaneous deposition rates in the range of 0.6–0.7 nm/s were determined with the two-color laser interferometer. The thickness of the deposited film (730 nm) determined by the FWII and the two-color laser interferometer was verified by the *ex situ* multiwavelength ellipsometry.

#### 4. CONCLUSIONS

An *in situ* single point two-color laser interferometer is used to monitor, in real time, the thickness of thin transparent films during plasma processing. The rate of change of film thickness is determined instantaneously by comparing the measured and modeled laser reflectance interference from the film and the substrate. The use of two different laser wavelengths provides higher accuracy of the calculated rates and a clear distinction between film etching and deposition. The film thickness is uniquely determined from the phase difference in the reflected laser intensity between the two laser colors and the measured etch rates. The local rate information is complemented by an *in situ* FWII, which uses a single wavelength of the plasma light emission to determine the uniformity of the average process rates across the substrate. The post-process analysis of the FWII data requires a couple of fringes to determine the average process rates, which may not be available for thin films of less than a single fringe. Also, the relatively fast response of the two-color laser interferometer to changes in the process rates makes it a desirable sensor for real-time process characterization and control. The combination of both sensors provides real-time instantaneous local information of film thickness, etch or growth rates, and global average uniformity of the process.

#### ACKNOWLEDGMENTS

The authors would like to thank P. Sandstrom for the construction of the electronic circuits used for computer control of the MCICP tool and for data acquisition. We thank R. Parker for his technical assistance with the MCICP tool and the optical setup. This work was supported by the National Science Foundation under Grant No. EEC-8721545.

#### REFERENCES

1. H. H. Busta, *Proc. Soc. Photo-opt. Instrum. Eng.* **276**, 164 (1981).
2. P. J. Marcoux and P. D. Foo, *Proc. Soc. Photo-opt. Instrum. Eng.* **276**, 170 (1981).
3. M. Sternheim, W. Van Gelder, and A. W. Hartman, *J. Electrochem. Soc.* **130**, 66 (1983).

4. G. Bruno, P. Capezzuto, G. Cicala, and F. Cramarossa, *Plasma. Chem. and Plasma Process.* **6**, 109 (1986).
5. B. R. Stoner, B. E. Williams, S. D. Walter, K. Niskimura, and J. T. Glass, *J. Mater. Res.* **7**, 257 (1995).
6. V. M. Donnelly, D. L. Flamm, W. C. Dautremont-Smith, and D. J. Werder, *J. Appl. Phys.* **55**, 242 (1984).
7. T. L. Vincent, P. P. Khargonekar, and F. L. Terry, *Diagnostic Techniques for Semiconductor Material Processing II*, S. W. Pang *et al.* (eds), Material Research Society, 87 (1996).
8. T. L. Vincent, P. P. Khargonekar, and F. L. Terry, *IEEE Trans. Semiconductor Manufacturing*, **10** (1997).
9. I. Tepermeister, W. T. Conner, T. Alzaben, H. Barnard, K. Gehlert, and D. Scipione, *Solid State Technol.* p. 63 (1996).
10. C. Lai, B. Brummmeir, and R. C. Woods, *J. Vac. Sci. Technol.* **A13**, 2086 (1995).
11. O. S. Heavens, *Optical Properties of Thin Solid Films*, Dover Publications, New York (1991). Republication of original text London: Butterworths Scientific Publications (1955).
12. P. A. Heimann and R. J. Schutz, *J. Electrochem. Soc.* **131**, 881 (1984).
13. C. D. Zuiker, D. M. Greun, and A. R. Krauss, *MRS Bull.* **XX**, 29 (1995).